Bioorganic & Medicinal Chemistry 18 (2010) 5071–5080

Contents lists available at ScienceDirect

Bioorganic & Medicinal Chemistry

journal homepage: www.elsevier.com/locate/bmc

Morphinans and isoquinolines: Acetylcholinesterase inhibition, pharmacophore modeling, and interaction with opioid receptors

Daniela Schuster [a], Mariana Spetea [a,b], Melisa Music [c], Silvia Rief [a], Monika Fink [a], Johannes Kirchmair [a], Johannes Schütz [a,b], Gerhard Wolber [a,d], Thierry Langer [a,d], Hermann Stuppner [c], Helmut Schmidhammer [a], Judith M. Rollinger [c,*]

[a] Department of Pharmaceutical Chemistry, Institute of Pharmacy, University of Innsbruck and Center for Molecular Biosciences Innsbruck—CMBI, Innrain 52a/c, A-6020 Innsbruck, Austria
[b] AlcaSynn Pharmaceuticals GmbH, Life Science Center, Mitterweg 24, A-6020 Innsbruck, Austria
[c] Department of Pharmacognosy, Institute of Pharmacy, University of Innsbruck and Center for Molecular Biosciences Innsbruck—CMBI, Innrain 52c, A-6020 Innsbruck, Austria
[d] Inte:Ligand Softwareentwicklungs-und Consulting GmbH, Clemens Maria Hofbauer-Gasse 6, A-2344 Maria Enzersdorf, Austria

ARTICLE INFO

Article history:
Received 1 March 2010
Accepted 26 May 2010
Available online 2 June 2010

Keywords:
Morphinans
Acetylcholinesterase inhibition
Opioid receptor
Pharmacophore modeling

ABSTRACT

Following indications from pharmacophore-based virtual screening of natural product databases, morphinan and isoquinoline compounds were tested in vitro for acetylcholinesterase (AChE) inhibition. After the first screen, active and inactive compounds were used to build a ligand-based pharmacophore model in order to prioritize compounds for biological testing. Among the virtual hits tested, the enrichment of actives was significantly higher than in a random selection of test compounds. The most active compounds were biochemically tested for their activity on μ, δ, and κ opioid receptors.

1. Introduction

In a society with a continuous increase of the population of over 65 years of age, a dramatic increase of dementia is observed. The age-specific prevalence of dementia is approximately 1.5% in persons aged 60–69 years and almost doubles every five years until it reaches 40% in nonagenarians.[1] One consequence of the rapid increase in the aging population worldwide is that the estimated 25 million people that are currently affected by dementia will double every 20 years. The most common manifestation of dementia—Alzheimer's disease (AD)—accounts for up to 75% of all dementia cases.[2]

The main cause of the loss of cognitive functions in AD patients is a continuous decline of the cholinergic neurotransmission in cortical and other regions of the human brain. At the molecular level, cholinergic neurotransmission is mediated by the neurotransmitter acetylcholine (ACh) which is rapidly hydrolyzed after its presynaptic release by acetylcholinesterase (AChE). Besides its well-known role in terminating synaptic transmission, AChE has been found to be involved in a number of other functions. For example, AChE is a factor in neurite growth and in accelerating the assembly of β-amyloid into amyloid fibrils which are characteristically found in the brain cells of AD patients.[3] A therapy with AChE inhibitors leads to a symptomatic amelioration of memory, cognition, mood, and daily living skills. Numerous studies confirm the vital role of this medication corresponding to the 'cholinergic hypothesis of learning'.[4] AChE inhibition is an approved strategy to raise ACh concentration and thereby increase the cholinergic function in the brain. So far, four AChE inhibitors have been approved by the European and US regulatory authorities for mild degenerative diseases: tacrine (**1**; Cognex®), donepezil (**2**; Arizept®), galanthamine (**3**; Reminyl®) and rivastigmine (4; Exelon®) (Chart 1).

Tacrine (**1**) and donepezil (**2**) are of synthetic origin while galanthamine (**3**) is a natural product from the genus *Galanthus* (Amaryllidaceae). Rivastigmine (**4**) is structurally closely related to physostigmine that is a prototype AChE inhibitor from the seeds of *Physostigma venenosum* (Papilionaceae). Another alkaloid from the plant kingdom—huperzine A from the clubmoss *Huperzia serrata* (Lycopodiaceae)—has been approved as drug for AD treatment in the People's Republic of China.[5] Apart from these natural products, numerous naturally occurring compounds that inhibit AChE have been identified.[6]

As can be seen from this example, nature is a rich source of bioactive compounds that can be used directly as drugs or as lead compounds for drug development. Over the last 25 years, 66% of all new chemical entities that were approved as drugs were natural

* Corresponding author. Tel.: +43 512 507 5308; fax: +43 512 507 2939.
E-mail address: Judith.Rollinger@uibk.ac.at (J.M. Rollinger).

0968-0896/$ - see front matter © 2010 Elsevier Ltd. All rights reserved.
doi:10.1016/j.bmc.2010.05.071

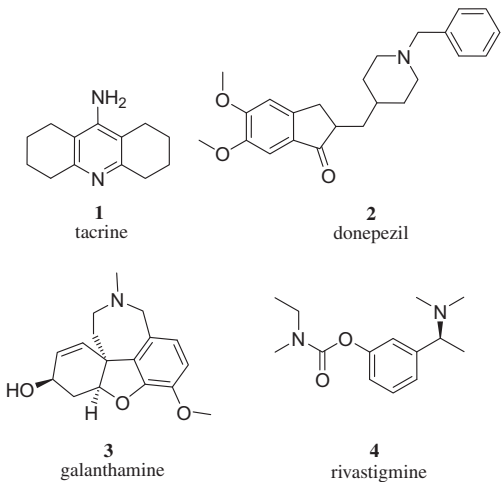

Chart 1. Clinically used AChE inhibitors.

products, natural product derivatives, synthetic compounds mimicking natural products, or compounds derived from a natural products-based pharmacophore.[7] In parallel, computer-based methods assisting drug discovery and development have rapidly evolved over the last 40 years.[8] Virtual screening (VS) has become an established method for selection and prioritization of compounds for biological evaluation. Applications and success stories have been reviewed recently.[9–13] In our working group, we have established an interface between the valuable resource of natural products and the powerful VS technology by the generation of two natural products 3D databases. The first database—the so-called DIOS database—consists of 9676 structures from medicinal plants described in the ancient ethnopharmacological source De materia medica by Pedanios Dioscorides (1st cent AD). The second database—the 'natural products database' (NPD)—includes over 110,000 compounds within a molecular mass between 140 and 700 Da.[14] These databases have been successfully mined for cyclooxygenase inhibitors,[14,15] acetylcholinesterase inhibitors,[16–18] human rhinovirus coat protein inhibitors,[19] and influenza virus neuraminidase inhibitors.[20]

In our first study on AChE inhibitors,[16] a structure-based pharmacophore model was generated based on the X-ray crystal structure of galanthamine in complex with *Torpedo californica* AChE (PDB entry 1qti,[21] Fig. 2). This model was used to virtually screen the NPD. Biological testing of non-alkaloid virtual hits led to the successful discovery of the new AChE inhibitors scopolin and scopoletin. Apart from these coumarin derivatives, some opioids from *Papaver somniferum*, for example, ethylmorphine, were predicted as active hits. In addition to these findings, in 1986, a study by Sim and Chua reported opioids of the morphinan-type as AChE inhibitors (Supplementary data, Chart S-1).[22] However, only 15 compounds were evaluated in this study and no further studies elaborating a structure–activity relationship of morphinan-based AChE inhibitors were

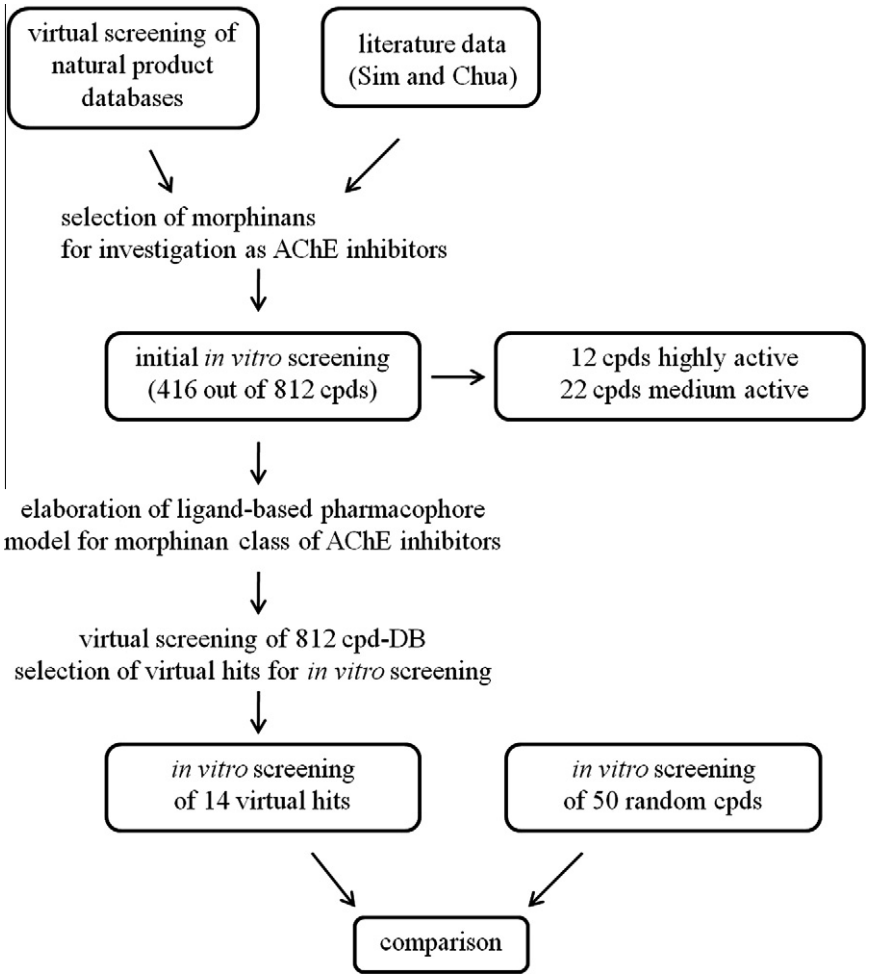

Figure 1. Study workflow for the identification of morphinan-type AChE inhibitors and elaboration of a pharmacophore model for enhancing the discovery of active compounds.

reported in literature. In addition, the K_i values for the reported morphinans indicated only moderate potency (12–109 μM). Both the results from virtual screening and the publication by Sim and Chua encouraged the further exploration of the effect of morphinan derivatives and related scaffolds on AChE activity.

2. Results and discussion

2.1. Study design

Following the strong indications from our virtual screening results of natural product databases with an established pharmacophore model for AChE inhibitors (1qti-based model) and the results from Sim and Chua,[22] morphinans were chosen for biological evaluation concerning AChE inhibition. Initially, 416 out of 812 compounds from an in-house database were evaluated for their AChE inhibitory activity using a spectrophotometric enzyme assay.[23] The resulting data were used to build a morphinan-focused ligand-based pharmacophore model for AChE inhibitors. This model was used to select 14 additional compounds for biological testing out of the in-house morphinan database. In parallel, further 50 compounds were chosen randomly for in vitro screening. Finally, the results of these screening runs were compared for validating the in silico-guided approach. An overview of the study workflow is presented in Figure 1.

2.2. Virtual hits from screening the natural products databases

The pharmacophore model derived from the PDB entry 1qti (Fig. 2) was used for screening the DIOS and NPD.

Screening of the DIOS returned overall 612 hits of which 45 had a high BestFit value of $\geqslant 3$. Three of these highly ranked hits were morphinan compounds: ethylmorphine, 10-oxocodeine, and 14β-hydroxycodeine. For all these compounds, no data on AChE activity were reported in literature. The NPD hitlist comprised 9763 hits of which 2455 were top ranked with BestFit values of $\geqslant 3$. The six morphinans present in this hitlist were oripavine, codeine, dihydrocodeine, 14β-hydroxycodeine, neopine, and morphine.

2.3. AChE inhibition by crude opium

As a first confirmation of the results of Sim and Chua[22] as well as of our virtual hits, crude opium was tested on its AChE inhibitory activity using a spectrophotometric assay with Ellman's reagent.[23] At a concentration of 100 μg/ml, AChE was inhibited to an extent of 50.4 ± 6.2%.

2.4. AChE inhibition by in-house compounds

As a consequence of the first promising results, 416 morphinan and non-morphinan compounds (e.g., isoquinolines) that were readily available at the time of this study were tested at a concentration of 500 μM using the spectrophotometric assay.[23] As positive control, the activity of galanthamine (**3**; IC_{50} = 3.2 ± 1.0 μM) was used. Compounds that inhibited AChE more than 50% are given in Figure 3.

2.5. Pharmacophore modeling, virtual screening, and model validation

As a tool for the further investigation of morphinans as AChE inhibitors, the suitability of the 1qti-model was tested. For this purpose, a 3D database of 812 compounds that were already available in-house was generated (for details see Section 4). This database mainly consisted of morphinans (n = 542) and morphinan-based compounds (157 indolomorphinans, 23 benzofuromorphinans, 10 dimeric morphinans, and 11 bimorphinans). In addition, it comprised 25 isoquinolines and 44 compounds from other chemical scaffolds. Screening the in-house database with the 1qti-based pharmacophore model in rigid mode resulted in a hitlist of 44 hits including morphine. Although over 20% of all virtual hits showed an activity in our in vitro assay (Table 2), we missed the most potent morphinan inhibitor in our hitlist, compound **5**.

For comparison, we generated a ligand-based pharmacophore model based exclusively on morphinan compounds identified in our study. The HipHop refine algorithm of Catalyst 4.11 was employed for model generation. This algorithm does not only compute the overlay of chemical features active compounds have in common, but also considers the spatial extension of inactive compounds from the training set. For example, an active compound with a methyl substituent at a defined position and an inactive compound with a propyl substituent at the same or a neighboring position would provoke the positioning of exclusion volume spheres (forbidden areas for the ligand) lining the coordinates corresponding to the methyl group. A good composition of the training set is crucial for representative model generation. Ideally,

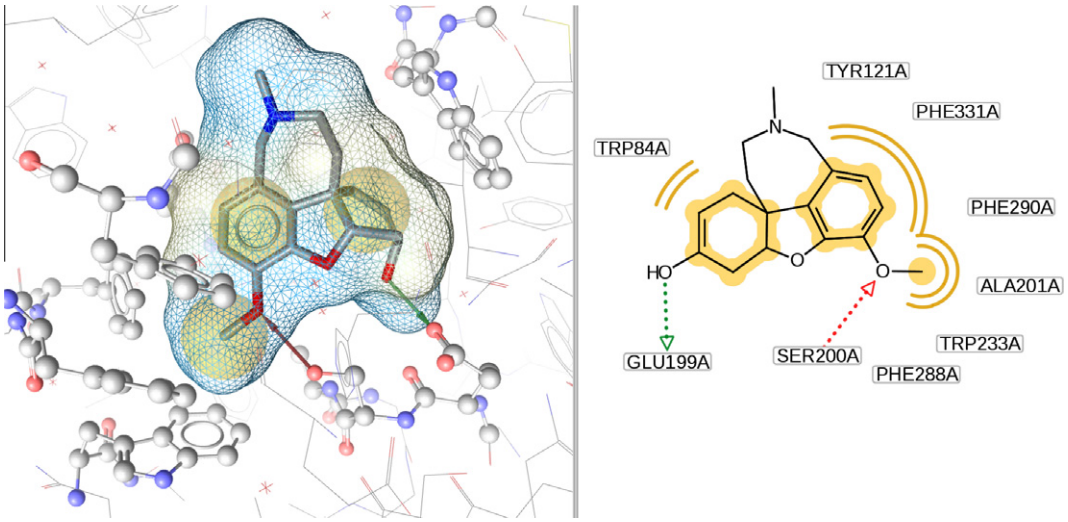

Figure 2. Pharmacophore model derived from the PDB entry 1qti (galanthamine complexed to *Tc*AChE). Chemical features are style- and color-coded: hydrophobic feature—yellow, hydrogen bond acceptor—red, hydrogen bond donor—green, shape restriction—wireframe. The hydrophobic feature on the 3-methoxy group was not included in the model employed for virtual screening.

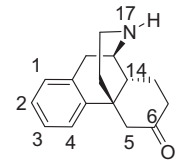

5 $R_4 = OCH_3$, $R_{17} = allyl$ — $IC_{50} = 1.0\ \mu M$
6 $R_4 = OH$, $R_{14} = OEt$, $R_{17} = CH_3$ — $IC_{50} = 37.1\ \mu M$
7 $R_4 = OCH_3$, $R_{14} = OCH_3$, $R_{17} = CH_3$ — $IC_{50} = 46.2\ \mu M$
8 $R_4 = OCH_3$, $R_{14} = OCH_3$, $R_{17} = allyl$ — $IC_{50} = 81.9\ \mu M$
9 $R_1 = OH$, $R_4 = OH$, $R_{17} = CHO$ — $IC_{50} = 105.1\ \mu M$
10 $R_4 = OCH_3$, $R_{14} = OH$, $R_{17} = allyl$ — 78 % inhibition
11 $R_{17} = CH_3$ — 74 % inhibition
12 $R_4 = OCH_3$, $R_{14} = OH$, $R_{17} = CH_3$ — 73 % inhibition
13 $R_4 = OCH_3$, $R_{17} = CH_2$-cPr — 70 % inhibition
14 $R_4 = OH$, $R_{14} = OCH_3$, $R_{17} = CH_3$ — 68 % inhibition
15 $R_4 = OH$, $R_{17} = allyl$ — 66 % inhibition
16 $R_4 = OCH_3$, $R_{17} = CH_2$-cBu — 64 % inhibition
17 $R_1 = A$, $R_{17} = CH_3$ — 64 % inhibition
18 $R_1 = OH$ — 59 % inhibition
19 $R_4 = OBu$, $R_{14} = OCH_3$, $R_{17} = CH_2$-cPr — 59 % inhibition
20 $R_4 = OCH_3$, $R_6 = (R)$-OH, $R_{17} = CH_2$-cBu — 57 % inhibition
21 $R_4 = OCH_3$, $R_{14} = OCH_3$ — 55 % inhibition
22 $R_1 = OCH_3$, $R_{17} = CH_3$ — 51 % inhibition
23 $R_4 = OCH_3$ — 50 % inhibition
24 $R_2 = OH$, $R_{17} = CH_3$ — 50 % inhibition

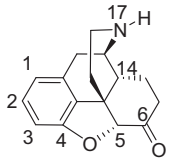

25 $R_3 = OCH_3$, $R_{14} = OH$, $R_{17} = CH_3$ — $IC_{50} = 76.2\ \mu M$
26 $R_3 = OH$, $R_{14} = OCH_3$, $R_{17} = CH_3$ — 84 % inhibition
27 $R_3 = OH$, $R_5 = CH_3$, $R_{14} = OCH_2CH_3$, $R_{17} = CH_3$ — 83 % inhibition
28 $R_3 = OH$, $R_{14} = OCH_3$, $R_{17} = (CH_3)_2$ — 75 % inhibition
29 $R_3 = OCH_3$, $R_6 = =NNHCONH_2$, $R_{14} = OCH_3$, $R_{17} = CH_3$ — 68 % inhibition
30 $R_{14} =$ phenylpropyl — 61 % inhibition
31 $R_3 = A$, $R_{14} = OH$, $R_{17} = CH_3$ — 56 % inhibition
32 $R_{14} = OCH_3$ — 55 % inhibition

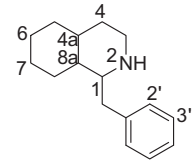

33 Δ1,2, $R_6 = OCH_3$, $R_{3'} = OH$ — $IC_{50} = 43.1\ \mu M$
34 Δ4a,8a, Δ6,7, $R_6 = OCH_3$, $R_{2'} = OH$ — $IC_{50} = 138.5\ \mu M$
35 Δ4a,8a, Δ6,7, $R_6 = OCH_3$, $R_{3'} = OH$ — 55 % inhibition
36 Δ4a,8a, $R_{2'} =$ O-benzyl — 50 % inhibition

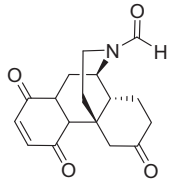

37 $IC_{50} = 12.7\ \mu M$

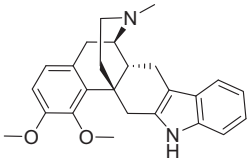

38 61 % inhibition

Figure 3. Compounds with AChE inhibition higher than 50% from the initial in vitro screen ($c = 500\ \mu M$; $n = 416$). For compounds with AChE inhibitory activity higher than 85% the IC_{50} value is given. Tables with full chemical structures are available as Supplementary data (Tables S-1 and S-2).

Table 1
Training set for the generation of the HipHop refine model

Compound	Group	Class
5	Highly active	2
6	Highly active	2
7	Active	1
8	Active	1
9	Active	1
26	Active	1
47	Inactive	0
49	Inactive	0
S-1	Inactive	0
S-2	Inactive	0
S-3	Inactive	0
S-4	Inactive	0
S-5	Inactive	0
S-6	Inactive	0
S-7	Inactive	0
S-8	Inactive	0
S-9	Inactive	0
S-10	Inactive	0
S-11	Inactive	0
S-12	Inactive	0
S-13	Inactive	0
S-14	Inactive	0
S-15	Inactive	0
S-16	Inactive	0

2D structures of the inactive compounds are available as Supplementary data, Table S-1.

compounds of different activity from the same chemical scaffold are included in the training set. The exact activity of the training compounds is not necessary for hypothesis generation. Instead, an activity class is assessed to each compound. Compounds from class 2 are highly active, class 1 indicates active compounds, and class 0 includes inactives used for model generation. The training set for our HipHop refine model is given in Table 1.

The hypothesis generation process returned ten models which were evaluated for their ability to find actives and exclude inactives from our 3D database of in-house compounds. The best model (Fig. 4) retrieved 32 hits (using rigid search) from the in-house database including compound **5** and morphine. Compared to the 1qti-model, the enrichment of actives raised considerably. Mining of the in-house database using flexible search led to a hitlist with 71 hits. Although the enrichment of highly and medium actives was less pronounced than in the hitlist from the rigid search, it still performs better than the 1qti-model (Table 2).

As a further validation of the model, 14 virtual hits from the database which have not been tested on their AChE-inhibiting effects were submitted to the spectrophotometric assay. For comparison, a random set of 50 compounds, which was not retrieved as virtual hits, was selected from the in-house database and also screened with our assay.

Although both approaches—the virtual screening and the random method—led to the identification of new AChE inhibitors

Table 2
Retrieval of hits from the in-house database (n = 812) using the AChE pharmacophore models

Activity class	1qti-model rigid search	1qti-model flexible search	Ligand-based model rigid search	Ligand-based model flexible search
Number of hits	44	49	32	71
Highly active[a]	2 (4.5%)	2 (4.1%)	4 (12.5%)	7 (9.9%)
Medium active[b]	2 (4.5%)	3 (6.1%)	7 (21.9%)	12 (16.9%)
Weakly active[c]	6 (13.6%)	6 (12.2%)	2 (6.3%)	6 (8.5%)
Inactive[d]	14 (31.8%)	16 (32.7%)	8 (25%)	22 (31.0%)
Unknown	20 (45.5%)	22 (44.9%)	11 (34.4%)	24 (33.8%)

[a] >80% inhibition at a concentration of 500 μM.
[b] 50–80% inhibition at a concentration of 500 μM.
[c] 30–50% inhibition at a concentration of 500 μM.
[d] Inhibition not detectable or <30% inhibition at a concentration of 500 μM.

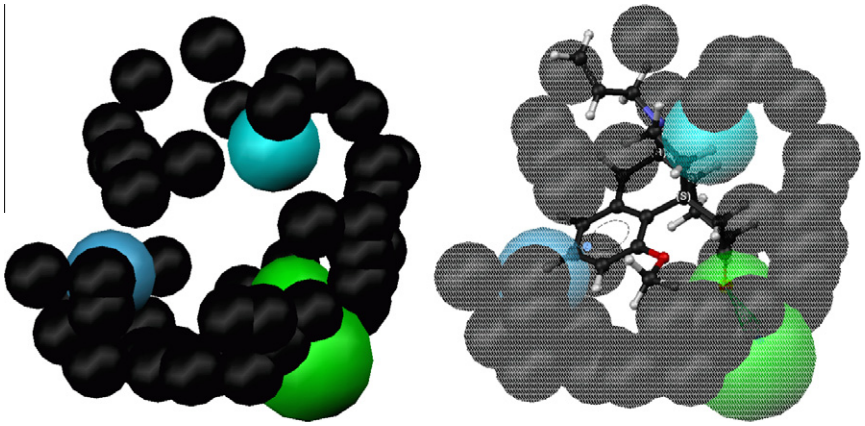

Figure 4. HipHop refine model for AChE inhibitors from the morphinan class (left). The model consists of one hydrogen bond acceptor (green), one hydrophobic feature (cyan), one hydrophobic aromatic feature (blue), and 54 exclusion volume spheres (black). Compound **5** fitted into the model (right).

(Tables 3 and 4), the enrichment of actives was superior for the virtual screening runs (Table 5).

Overall, 14 out of a total of 481 tested compounds (3.1%) showed AChE inhibition of at least 80%. This proportion is accurately reflected by the fraction of highly active hits identified in the initial in vitro screening (11 out of 416 compounds, 2.6%) and the random in vitro screening (1 out of 50 compounds, 2.0%) that was carried out in parallel to the pharmacophore-based selection. In order to quantitatively assess the quality of the pharmacophore models, enrichment factors (EFs) were calculated (Table 6).

2.6. Chemistry

The syntheses of **47** and **49**, which have been used in the training set for the pharmacophore model, have not been previously reported. Compound **47** has been prepared from 5β-methyldihydrothebainone[24,25] by alkylation with 5-chloro-1-phenyl-1*H*-tetrazole in DMF (Scheme 1). Catalytic hydrogenation of 3-benzyloxy-14-ethoxy-4-methoxy-*N*-methylmorphinan-6-one[26] in MeOH afforded **49** (Scheme 2). Details of these synthetical procedures are described in the Section 4.

Table 3
AChE inhibition by virtual hits (n = 14) from the in-house database derived from a flexible search using the ligand-based model

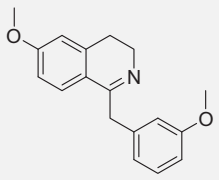

39
86% Inhibition[a]
IC_{50} = 42.9 ± 8.3 μM

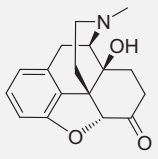

40
86% Inhibition
IC_{50} = 65.3 ± 11.3 μM

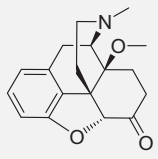

41
73% Inhibition
IC_{50} = 140.1 ± 18.3 μM

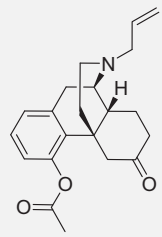

42
72% Inhibition
IC_{50} = 193.4 ± 25.5 μM

Only hits with an AChE inhibition of at least 50% are shown.
[a] % inhibition measured at a concentration of 500 μM.

Table 4
AChE inhibition by random compounds not included in our virtual hitlist ($n = 50$)

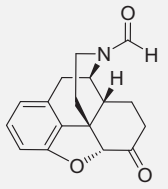

43
94% Inhibition
IC_{50} = 60.3 ± 16.6 μM

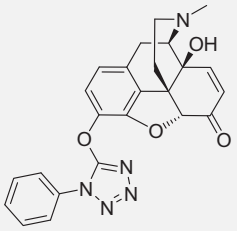

44
56% Inhibition

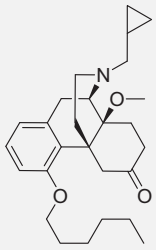

45
51% Inhibition
IC_{50} = 404.6 ± 83.1 μM

Only hits with an AChE inhibition of at least 50% are shown.
[a] % inhibition measured at a concentration of 500 μM.

Table 5
Novel AChE inhibitors selected from the pharmacophore-based search vs. random selection

Activity class	Pharmacophore-based selection	Random selection
Number of tested compounds	14	50
Highly active[a]	2 (14.3%)	1 (2.0%)
Medium active[b]	2 (14.3%)	2 (4.0%)
Weakly active[c]	4 (28.6%)	4 (8.0%)
Inactive[d]	6 (42.9%)	43 (86.0%)

[a] >80% inhibition at a concentration of 500 μM.
[b] 50–80% inhibition at a concentration of 500 μM.
[c] 30–50% inhibition at a concentration of 500 μM.
[d] Inhibition not detectable or <10% inhibition at a concentration of 500 μM.

Table 6
Enrichment factors for the 1qti-model and the ligand-based pharmacophore model

Model	1qti-model rigid search	1qti-model flexible search	Ligand-based model rigid search	Ligand-based model flexible search
TP (highly actives in the hitlist)	2	2	5	9
n (hitlist size)	44	49	32	71
A (number of actives in the database)	14	14	14	14
N (database size)	481	481	481	481
EF	1.56	1.40	5.37	4.36

The calculations are based on the retrieval of highly active compounds (AChE inhibition >80%) from the dataset.

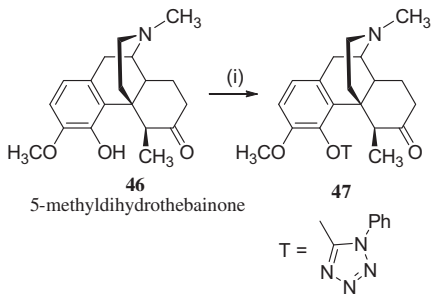

46
5-methyldihydrothebainone

47

Scheme 1. Reagents and conditions: (i) 5-Chloro-1-phenyl-1*H*-tetrazole, K_2CO_3, DMF, rt, 72 h.

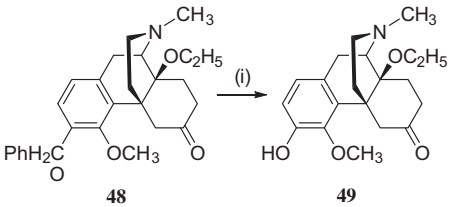

48 **49**

Scheme 2. Reagents and conditions: (i) Catalytic hydrogenation, 10% Pd/C, MeOH, 30 psi, rt, 3 h.

2.7. Molecular docking study

The binding mode of the most potent AChE inhibitor identified in our study—compound **5**—was predicted by docking experiments using GOLD 3.1.[27] For validation of the docking settings (see Section 4), galanthamine was docked into the binding site of 1qti which yielded satisfying results (Supplementary data, Fig. S-2). Subsequent docking of compound **5** revealed a similar binding site of **5** and galanthamine (**3**); however, different interaction patterns were predicted for the two ligands (Fig. 5). Common protein–ligand interactions for these compounds essentially included the basic nitrogen positioned in an aromatic cage. While galanthamine directly forms hydrogen bonds with the catalytically active amino acid residues Glu199 and Ser200, no such interactions were predicted for compound **5**. In contrast, a hydrogen bond was observed to Tyr130.

The predicted binding interactions of **5** with AChE were compared to the HipHop refine model. The docking solution of **5** was imported into the PDB structure 1qti and submitted to pharmacophore model generation using LigandScout.[28] Of course, the docked compound established more than three chemical interactions with the protein; however, a reduction of chemical features led to a model closely resembling the ligand-based HipHop refine model. It also consisted of hydrophobic features representing the aromatic ring and the bridging ring. A hydrogen bond was established between the 6-keto group and Tyr130 (Fig. 5).

2.8. Opioid receptor binding

Among the investigated morphinan and isoquinoline compounds, some of the most active AChE inhibitors (inhibition ⩾80%) identified in this study were further evaluated in in vitro receptor binding assays for the interaction with μ, δ, and κ opioid receptors.[29] The binding affinities at μ and δ opioid receptors were determined by inhibition of binding of [^{3}H][D-Ala^2,Me-Phe^4,Gly-ol^5]enkephalin ([^{3}H]DAMGO) and [^{3}H][Ile^{5,6}]deltorphin II to rat

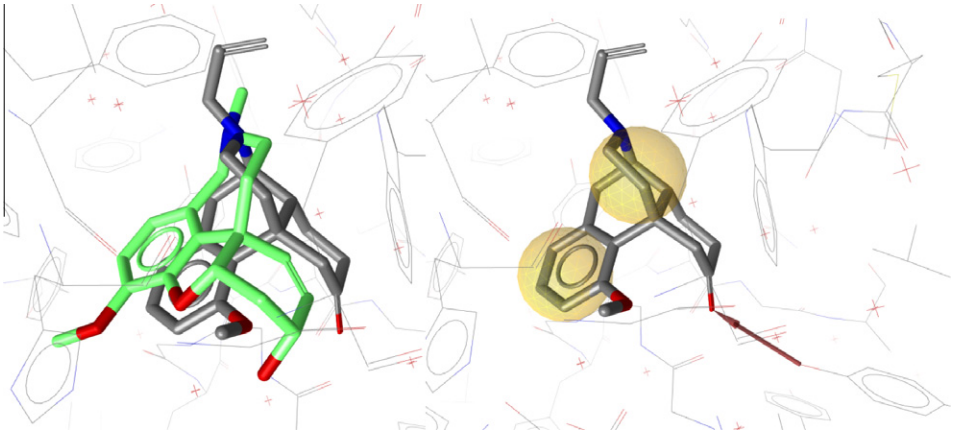

Figure 5. Left: Overlay of galanthamine (green; based on the PDB entry 1qti) with the top-ranked docked binding position of compound **5**. Right: Some predicted interactions observed for **5** with the active site of AChE closely resemble the ligand-based pharmacophore model (compare to Fig. 1).

brain membranes. The affinities of the target compounds at κ opioid receptors were determined by displacement of [^{3}H]U69,593 using guinea pig brain membranes. The μ, δ and κ opioid receptor binding affinities expressed as inhibition constant (K_i) are summarized in Tables 7 and 8. The selectivity for the μ opioid receptor versus δ and κ receptors was defined by the ratio of the K_i values. For comparison purposes, the opioid binding affinity data for morphine and oxycodone (compound **25**) are also included.

The two isoquinoline compounds identified in this study to display potent inhibitory activity of AChE (inhibition ⩾80%) showed low or no binding to the μ, δ and κ opioid receptors (Table 8).

Table 8
Opioid receptor binding affinities of isoquinoline compounds

Compound	K_i (nM) ± SEM		
	μ opioid receptor [^{3}H]DAMGO[a]	δ opioid receptor [^{3}H][Ile^{5,6}]deltorphin II[a]	κ opioid receptor [^{3}H]U69,593[b]
33	2318 ± 209	>10,000	>10,000
34	>10,000	>10,000	>10,000

[a] Rat brain membranes were used.
[b] Guinea pig brain membranes were used.

2.9. Structure–activity relationship

Following the pattern of SAR, all morphinan compounds having a *N*-methyl and *N*-allyl group in position 17 specifically bound to the opioid receptors displaying selectivity for the μ opioid receptor (Table 7). In contrast, the *N*-formyl substituted morphinans **9**, **37**, and **43** showed no specific binding to any of the three opioid receptor types (K_i >10 μM). Thus, the presence of a formyl group in position 17 significantly alters the interaction with opioid receptors.

As expected and in agreement with the previous determinations of the positive influence of 14-alkoxy substituents in *N*-methyl-morphinan-6-ones[30,33–38] such as 14-methoxy derivatives, **7** and **26**, and 14-ethoxy derivatives, **6** and **27**, showed high μ opioid receptor affinity and selectivity, with K_i values ranging between 0.10 and 2 nM (Table 7). The *N*-methyl substituted compounds displayed a 6- to 65-fold enhanced affinity to the μ binding site in comparison to morphine (K_i = 6.55 nM) and a 22- to 95-fold higher μ receptor affinity than compound **25** (K_i = 43.6 nM). Regarding the AChE inhibitory activity, no major difference in the potency was observed between the 14-methoxy and 14-ethoxy substituted *N*-methyl-14-alkoxymorphinans (IC_{50} of 37.1 μM for **6** and 46.2 μM for **7**, Fig. 3).

The *N*-allyl substituted morphinan-6-ones, compounds **5** and **8** showed both decreased μ opioid receptor affinity and selectivity,

Table 7
Opioid receptor binding affinities of morphinan compounds

Compound	K_i (nM) ± SEM			Selectivity ratio	
	μ opioid receptor [^{3}H]DAMGO[a]	δ opioid receptor [^{3}H][Ile^{5,6}]deltorphin II[a]	κ opioid receptor [^{3}H]U69,593[b]	δ/μ	κ/μ
Morphine[c]	6.55 ± 0.74	217 ± 19	113 ± 9[a]	33	17
5	20.2 ± 1.2	316 ± 26	33.1 ± 1.6	16	2
6	1.15 ± 0.01	101 ± 14	403 ± 80	88	350
7	2.00 ± 0.08	210 ± 7	567 ± 15	105	284
8	67.2 ± 1.3	1253 ± 2	328 ± 22	19	5
9	>10,000	>10,000	>10,000	1	1
25[d]	43.6 ± 1.5	1087 ± 246	2658 ± 367[a]	25	61
26[e]	0.10 ± 0.01	4.80 ± 0.22	10.2 ± 2.0[a]	48	102
27[f]	0.46 ± 0.01	12.2. ± 1.8[f]	43.2 ± 5.7[a]	26	94
37	>10,000	>10,000	>10,000	1	1
43	>10,000	>10,000	>10,000	1	1

[a] Rat brain membranes were used.
[b] Guinea pig brain membranes were used.
[c] Data from Spetea et al. 2003.[29]
[d] Data from Spetea et al. 2005.[30]
[e] Data from Spetea et al. 2004.[31]
[f] Data from Fürst et al. 1993.[32]

being lower than that of morphine, or comparable to compound **25** (Table 7). The present receptor binding data for **8** are in agreement with the earlier report on opioid activities in the mouse vas deferens bioassay.[34]

When comparing *N*-methyl versus *N*-allyl 14-methoxy substituted morphinan-6-ones, **7** and **8**, it was apparent that the presence of an allyl group in position 17 leads to reduced affinity and selectivity for the μ opioid receptor. However, an *N*-allyl group is more favorable to an *N*-methyl group regarding the inhibitory potency of AChE activity (IC_{50} of 46.2 μM for **7** and 81.9 μM for **8**). On the other hand, the *N*-allyl 14-unsubstituted derivative compound **5** (IC_{50} of 1 μM) showed about 82-fold higher inhibitory activity of AChE compared to its 14-methoxy analogue **8** (Fig. 3), while both compounds display decreased μ opioid receptor affinity but comparable μ receptor selectivity (Table 7). It appears that the presence of a 14-methoxy group in this class of 4-methoxy substituted *N*-allymorphinans causes no major alterations in binding affinity and selectivity for μ sites.

A major impact of the substitution of positions 3 and 4—highly depending on the presence or absence of the 4,5-ether bridge—was observed: Opening of the 4,5-ether bridge in 3-deoxygenated morphinans results in compounds with enhanced AChE inhibition. In cases where positions 3 and 4 were both substituted (e.g., with two methoxy groups), AChE inhibitory activity was completely lost. Interestingly, compounds with a 4,5-ether bridge and a substituent in position 3 (e.g., **31**) could still inhibit AChE. Thus, it is hypothesized that ring opening and derivatization at position 4 leads to a steric clash of the ligand with the AChE binding site which in turn causes the inactivity of this compound.

N-Formylation in position 17 eliminates opioid activity of morphinans but not AChE inhibition (e.g., **43**, Fig. 3). Thus, the basic amine nitrogen in morphinans is not essential for AChE inhibition. The fact that the ionizable amine nitrogen was not reflected by a chemical feature in the ligand-based pharmacophore model supports this conclusion. The substituent in position 14 seems not to be crucial concerning AChE inhibition.

3. Conclusion

This is the first study that presents a large investigation of morphinan and isoquinoline compounds as AChE inhibitors. Starting from virtual screening hits, a series of AChE inhibitors were identified with activities in the low micromolar range. In parallel, a pharmacophore model was established that may serve as a useful tool to prioritize compounds for biological evaluation of their cholinergic enhancing properties and for future synthesis projects.[39]

4. Experimental

4.1. Spectrophotometric assay for AChE inhibitory activity

The AChE inhibitory activity was determined using a modified Ellman's method[23,40] with electric eel AChE (EC 3.1.1.7), acetylthiocholiniodide, and 5,5′-dithiobis-(2-nitrobenzoic acid): Sigma–Aldrich Chemie Gmbh, Steinheim, Germany; Galanthamine. HBr (Tocris; Cookson Ltd, Avonmouth UK Bristol)] served as the positive control in our assay (IC_{50} of 3.2 ± 1.0 μM) using a 96-well microplate assay as previously described.[16] The percentage of the enzyme inhibition was calculated by determining the rate in presence of inhibitor and the vehicle (containing 1% DMSO) compared to the rate in the control sample ($n = 4$) and analyzed with Student's *t*-test.

4.2. Chemistry

The required reagents as well as anhydrous DMF were purchased from Fluka, Switzerland in the highest purities available. The solvents were distilled before usage. Melting points were determined on a Kofler melting point microscope and are uncorrected. IR spectra were recorded with a Mattson Galaxy Series FTIR 3000 spectrometer (in cm^{-1}). ^1H NMR spectra were recorded on a Varian Gemini 200 (200 MHz) spectrometer. Chemical shifts (δ) are reported in ppm (relative to $SiMe_4$ as internal standard), coupling constants (J) in Hz. Mass spectra were recorded on a Finnigan Mat SSQ 7000 apparatus. Elemental Analyses were performed at the Institute of Physical Chemistry at the University of Vienna, Austria. For TLC, POLYGRAM SIL G/UV_{254} precoated plastic sheets (Macherey-Nagel, Germany) were used (eluent: CH_2Cl_2/MeOH/concentrated NH_4OH solution, 90:9:1), and for column chromatography, Silica Gel 60 (230–400 mesh ASTM, Fluka, Switzerland) was used. Oxycodone (**25**) was purchased from Fluka, Switzerland, as oxycodone hydrochloride solution (1 mg/mL ± 5% in methanol; purity of ⩾98%). Raw opium was used from the pharmacognostic collection *Dittrichiana*, Institute of Pharmacy/Pharmacognosy, University of Innsbruck, Austria.

4.2.1. 5β,17-Dimethyl-3-methoxy-4-[(1-phenyl-1*H*-tetrazol-5-yl)oxy]morphinan-6-one (47)

A mixture of 5β-methyldihydrothebainone[24,25] (3.8 g, 12.0 mmol), K_2CO_3 (3.8 g, 27.5 mmol) and 5-chloro-1-phenyl-1*H*-tetrazole (2.3 g, 12.7 mmol) in anhydrous DMF (20 mL) was stirred at room temperature for 72 h. After filtration, the filtrate was evaporated and the residue dissolved in AcOEt (20 mL), washed with H_2O (2 × 10 mL), dried (Na_2SO_4) and evaporated to give a crystalline residue (4.98 g) which was recrystallized from MeOH (5 mL) to yield 2.94 g (53%) of **47**. An analytical sample was obtained by recrystallization of a small amount from MeOH: mp 180–182 °C; IR (KBr): (C=O) 1700 cm^{-1}; ^1H NMR ($CDCl_3$) δ 7.66 (m, 5 arom H), 6.92 (d, $J = 8.0$, 1 arom H), 6.65 (d, $J = 8.0$, 1 arom H), 3.52 (s, CH_3O), 2.37 (s, CH_3N), 1.11 (d, $J = 7$, C5–CH_3). Anal. ($C_{26}H_{29}N_5O_3$) C, H, N.

4.2.2. 14-Ethoxy-3-hydroxy-4-methoxy-17-methylmorphinan-6-one (49)

A mixture of 3-benzyloxy-14-ethoxy-4-methoxy-17-methylmorphinan-6-one[26] (500 mg, 1.15 mmol), MeOH (60 mL) and 10% Pd/C catalyst (60 mg) was hydrogenated at 30 psi and room temperature for 3 h. The catalyst was filtered off and washed with MeOH, and the filtrate was evaporated. The residue (470 mg oil) was crystallized from MeOH (1 mL) to afford 402 mg (80%) of **49**: mp 209–211 °C; IR (KBr): (C=O) 1705 cm^{-1}; ^1H NMR ($CDCl_3$) δ 6.78 (d, $J = 8.0$, 1 arom H), 6.71 (d, $J = 8.0$, 1 arom H), 3.79 (s, CH_3O), 2.32 (s, CH_3N), 1.27 (t, $J = 6$, CH_2CH_3); CI-MS m/z 346 (M^++1). Anal. ($C_{20}H_{27}NO_4 \cdot 0.1MeOH$) C, H, N.

Elemental analysis data for both compounds are available as Supplementary data (Table S-4).

4.3. Molecular modeling and virtual screening

Molecular modeling studies were carried out on an Intel Pentium Core 2 Duo 6400 equipped with 1 GB RAM running Linux Fedora Core 6.

4.3.1. Data preparation

All compounds used in the in silico approach were generated within Catalyst Version 4.11[41] and submitted to conformational analysis using the 'best' option with a maximum of 250 conformers per molecule and a maximum conformer energy of 20 kcal/mol above the calculated energy minimum. The 3D database of in-house morphinan and isoquinoline compounds was generated using the catDB module of Catalyst. A maximum of 255 conformers per molecule was included into the database.

4.3.2. HipHop Refine pharmacophore model generation

The HipHop Refine algorithm of Catalyst generates a common feature pharmacophore model from compounds labeled as highly active from the training set. Chemical features considered in the hypothesis generation process were hydrogen bond acceptors, positively ionizable groups, hydrophobic, and hydrophobic aromatic features. In the first step—the constructive phase—a set of common feature models is generated. In a second step—the optimization phase—exclusion volume spheres are strategically placed where steric interactions contributing to biological (in-)activity can be approximated. This information is taken from the inactive compounds included in the training set. For example, if the compound ABC is active and ABCD is not active—even though ABCD contains the same pharmacophore as ABC—differences in the steric bulk are estimated to carry responsibility for the absence of ABCDs biological activity. At the 3D location of D, an exclusion volume sphere is placed.

4.3.3. Virtual screening

Screening of the DIOS and NPD using the 1qti-model was performed employing the fast (rigid) fitting algorithm of Catalyst 4.11.[41] Fit values were computed using best fit calculation which means that the ligand is minimized into the model before calculating the fit.

4.3.4. Enrichment factor (EF) calculation

The EF is a measure how well active compounds are found by the model in comparison to inactive compounds or decoys, that is, compounds that are supposed to be inactive. It is not only a measure how well the model finds highly active hits from the database, but also compares the fraction of actives from a hitlist with the ratio of actives/all compounds from the entire screening database. The EF is calculated using the equation[42,43]

$$\mathrm{EF} = \frac{\mathrm{TP}/n}{A/N}$$

where TP is the number of true positives (active hits) in the hitlist, n is the size of the hitlist, A is the number of active ligands in the entire database, and N is the number of all compounds in the entire database. For EF calculations, all 481 compounds for which the AChE inhibitory potency was evaluated in vitro were considered.

4.3.5. Docking

Docking experiments were performed employing GOLD 3.1.[27] The protein structure from the PDB entry 1qti was prepared for docking using Sybyl 8.0.[44] The co-crystallized ligand galanthamine was deleted from the file. Hydrogens were added using Sybyl's biopolymer tool. All water molecules included in the active site of the protein were set to 'toggle' and 'spin' using a perl script.[45] The cavity site was detected by the program GOLD using the coordinates of the co-crystallized galanthamine as starting point and allowing 20 Å around this area as location for the binding. As a validation for the docking, the bioactive conformation of galanthamine was also submitted to docking using the same settings. The starting conformation for compound **5** docking was a low-energy conformer generated using Catalyst's modified CHARMm force field-based 3D structure minimization.

4.4. Opioid receptor binding assay

Membrane fractions were prepared from Sprague–Dawley rat or guinea pig brains (Institut für Labortierkunde und Laborgenetik, Medizinische Universität Wien, Himberg, Austria) as previously described.[29] Binding experiments were performed in 50 mM Tris–HCl buffer (pH 7.4.) in a final volume of 1 ml containing 0.3–0.5 mg protein and different concentrations the test compound as described.[29] Rat brain membranes were incubated either with [^{3}H]DAMGO (Perkin–Elmer, Boston, MA, USA; 45 min, 35 °C) or [^{3}H][Ile^{5,6}]deltorphin II (Institute of Isotopes Co. Ltd, Budapest, Hungary; 45 min, 35 °C). Guinea pig brain membranes were incubated with [^{3}H]U69,593 (Perkin–Elmer, Boston, MA, USA; 30 min, 30 °C). Non-specific binding was determined in the presence of 10 μM unlabeled naloxone. Reactions were terminated by rapid filtration through Whatman glass fiber filters GF/B pretreated with 0.1% polyethylenimine ([^{3}H]U69,593) or GF/C ([^{3}H]DAMGO and [^{3}H][Ile^{5,6}]deltorphin II) using a Brandel M24R Cell Harvester, followed by three washings with 5 ml of ice-cold 50 mM Tris–HCl buffer (pH 7.4.). Inhibition constant (K_i) values were calculated from competition binding curves using GraphPad Prism (San Diego, CA, USA) program. The values are expressed as the mean ± S.E.M of 2–4 independent experiments, each performed in duplicate.

Acknowledgments

This study was granted by the Austrian Research Promotion Agency (FFG, Bridge Project 810059). We acknowledge the technical assistance of Beatrix Jungwirth.

Supplementary data

Supplementary data associated with this article can be found, in the online version, at doi:10.1016/j.bmc.2010.05.071.

References and notes

1. Qiu, C.; De Ronchi, D.; Fratiglioni, L. *Curr. Opin. Psychiatry* **2007**, *20*, 380.
2. Qiu, C.; Kivipelto, M.; von Strauss, E. *Dialogues Clin. Neurosci.* **2009**, *11*, 111.
3. Zhang, X. *Curr. Drug Targets CNS Neurol. Disord.* **2004**, *3*, 137.
4. Bartus, R. T.; Dean, R. L.; Beer, B.; Lipps, A. S. *Science* **1982**, *217*, 408.
5. Jiang, H.; Luo, X.; Bai, D. *Curr. Med. Chem.* **2003**, *10*, 2231.
6. Houghton, P. J.; Ren, Y.; Howes, M.-J. *Nat. Prod. Rep.* **2006**, *23*, 181.
7. Newman, D. J.; Cragg, G. M. *J. Nat. Prod.* **2007**, *70*, 461.
8. Ekins, S.; Mestres, J.; Testa, B. *Br. J. Pharmacol.* **2007**, *152*, 9.
9. Langer, T.; Wolber, G. *Pure Appl. Chem.* **2004**, *76*, 991.
10. Ekins, S.; Mestres, J.; Testa, B. *Br. J. Pharmacol.* **2007**, *152*, 21.
11. Kirchmair, J.; Distinto, S.; Schuster, D.; Spitzer, G.; Langer, T.; Wolber, G. *Curr. Med. Chem.* **2008**, *15*, 2040.
12. Langer, T.; Hoffmann, R. D. *Exp. Opin. Drug Discov.* **2006**, *1*, 261.
13. Villoutreix, B. O.; Renault, N.; Lagorce, D.; Sperandio, O.; Montes, M.; Miteva, M. A. *Curr. Protein Pept. Sci.* **2007**, *8*, 381.
14. Rollinger, J. M.; Haupt, S.; Stuppner, H.; Langer, T. *J. Chem. Inf. Comput. Sci.* **2004**, *44*, 480.
15. Rollinger, J. M.; Bodensieck, A.; Seger, C.; Ellmerer, E. P.; Bauer, R.; Langer, T.; Stuppner, H. *Planta Med.* **2005**, *71*, 399.
16. Rollinger, J. M.; Hornick, A.; Langer, T.; Stuppner, H.; Prast, H. *J. Med. Chem.* **2004**, *47*, 6248.
17. Rollinger, J. M.; Mock, P.; Zidorn, C.; Ellmerer, E. P.; Langer, T.; Stuppner, H. *Curr. Drug Discov. Technol.* **2005**, *2*, 185.
18. Schuster, D.; Kern, L.; Hristozov, D. P.; Terfloth, L.; Bienfait, B.; Laggner, C.; Kirchmair, J.; Grienke, U.; Wolber, G.; Langer, T.; Stuppner, H.; Gasteiger, J.; Rollinger, J. M. *Comb. Chem. High Throughput Screening* **2010**, *13*, 54.
19. Rollinger, J. M.; Steindl, T. M.; Schuster, D.; Kirchmair, J.; Anrain, K.; Ellmerer, E. P.; Langer, T.; Stuppner, H.; Wutzler, P.; Schmidtke, M. *J. Med. Chem.* **2008**, *51*, 842.
20. Grienke, U.; Schmidtke, M.; Kirchmair, J.; Pfarr, K.; Wutzler, P.; Dürrwald, R.; Wolber, G.; Liedl, K. R.; Stuppner, H.; Rollinger, J. M. *J. Med. Chem.* **2010**, *53*, 778.
21. Bartolucci, C.; Perola, E.; Pilger, C.; Fels, G.; Lamba, D. *Protein: Struct., Funct., Genet.* **2001**, *42*, 182.
22. Sim, M. K.; Chua, M. E. *Clin. Exp. Pharmacol. Physiol.* **1986**, *13*, 159.
23. Ellman, G. L.; Courtney, K. D.; Andres, V. J.; Featherstone, R. M. *Biochem. Pharmacol.* **1961**, *7*, 88.
24. Small, L.; Fitch, H. M.; Smith, W. E. *J. Am. Chem. Soc.* **1936**, *58*, 1457.
25. Schmidhammer, H.; Fritsch, F.; Burkard, W. P.; Eggstein-Aeppli, L.; Hefti, F.; Holck, M. I. *Helv. Chim. Acta* **1988**, *71*, 642.
26. Schmidhammer, H.; Jennewein, H. K.; Krassnig, R.; Traynor, J. R.; Patel, D.; Bell, K.; Froschauer, G.; Mattersberger, K.; Jachs-Ewinger, C.; Jura, P.; u.a. *J. Med. Chem.* **1995**, *38*, 3071.
27. The Cambridge Crystallographic Data Centre—CCDC: Cambridge, 2004–2008.
28. Wolber, G.; Langer, T. *J. Chem. Inf. Model.* **2005**, *45*, 160.
29. Spetea, M.; Tóth, F.; Schütz, J.; Ötvös, F.; Tóth, G.; Benyhe, S.; Borsodi, A.; Schmidhammer, H. *Eur. J. Neurosci.* **2003**, *18*, 290.

30. Spetea, M.; Greiner, E.; Aceto, M. D.; Harris, L. S.; Coop, A.; Schmidhammer, H. *J. Med. Chem.* **2005**, *48*, 5052.
31. Spetea, M.; Friedmann, T.; Riba, P.; Schütz, J.; Wunder, G.; Langer, T.; Schmidhammer, H.; Fürst, Z. *Eur. J. Pharmacol.* **2004**, *483*, 301.
32. Fürst, Z.; Búzás, B.; Friedmann, T.; Schmidhammer, H.; Borsodi, A. *Eur. J. Pharmacol.* **1993**, *236*, 209.
33. Schmidhammer, H.; Aeppli, L.; Atwell, L.; Fritsch, F.; Jacobson, A. E.; Nebuchla, M.; Sperk, G. *J. Med. Chem.* **1984**, *27*, 1575.
34. Schmidhammer, H.; Schratz, A.; Mittendorfer, J. *Helv. Chim. Acta* **1990**, *73*, 1784.
35. Schmidhammer, H. *Curr. Top. Med. Chem.* **1993**, *1*, 261.
36. Schütz, J.; Spetea, M.; Koch, M.; Aceto, M. D.; Harris, L. S.; Coop, A.; Schmidhammer, H. *J. Med. Chem.* **2003**, *46*, 4182.
37. Greiner, E.; Spetea, M.; Krassnig, R.; Schüllner, F.; Aceto, M. D.; Harris, L. S.; Traynor, J. R.; Woods, J. H.; Coop, A.; Schmidhammer, H. *J. Med. Chem.* **2003**, *46*, 1758.
38. Lattanzi, R.; Spetea, M.; Schüllner, F.; Rief, S. B.; Krassnig, R.; Negri, L.; Schmidhammer, H. *J. Med. Chem.* **2005**, *48*, 3372.
39. Rollinger, J. M.; Prast, H.; Schuster, D.; Langer, T.; Hornick, A.; Stuppner, H. Eur. Pat. Appl. EP 09015938.5.
40. Ingkaninan, K.; de Best, C. M.; van der Heijden, R.; Hofte, A. J. P.; Karabatak, B.; Irth, H.; van der Greef, J.; Veerpoorte, R. *J. Chromatogr., A* **2000**, *872*, 61.
41. Accelrys Software Inc.: San Diego, CA, USA, 2005–2009.
42. Jacobsson, M.; Liden, P.; Stjernschantz, E.; Bostroem, H.; Norinder, U. *J. Med. Chem.* **2003**, *46*, 5781.
43. Diller, D. J.; Li, R. *J. Med. Chem.* **2003**, *46*, 4638.
44. Tripos: St. Louis, MO, USA, 2008.
45. Schuster, D.; Maurer, E.; Laggner, C.; Nashev, L. G.; Wilckens, T.; Langer, T.; Odermatt, A. *J. Med. Chem.* **2006**, *49*, 3454.